An improved P-HEMT large-signal model for medium-power Ka-band amplifiers

M. Pirola, G. Ghione, J. M. Dortu†, J. Müller†

Dipartimento di Elettronica, Politecnico di Torino, Corso Duca degli Abruzzi 24, I-10129 Torino, ITALY
† SIEMENS Corporate Research and Development, Otto Hahn Ring 6, 81739 München, GERMANY

Abstract

A large-signal lumped-parameter model for pseudomorphic HEMT devices (P-HEMTs) is described. The model was implemented in the HARPE/OSA environment on the basis of the Angelov approach and further developed through comparison with three generations of SIEMENS P-HEMTs; an MDS version is also available. The final model shows very good agreement with experimental data for the DC and small-signal parameters on a wide range of bias points; preliminary comparisons carried out on large-signal measurements are also satisfactory.

Introduction

During the last few years, Pseudomorphic High Electron Mobility Transistors (P-HEMTs) have shown good performances not only in traditional low-noise applications, but also as medium-power devices. This has fostered the interest of the technical community towards the development of large-signal circuit-oriented lumped parameter models characterized through DC, small-signal and large signal measurements.

At first, attempts were made to apply to HEMTs the conventional MESFET built-in models made available by commercial large-signal harmonic-balance simulators, such as the Curtice, Curtice-Ettemberg and Materka models. Those early effort were only partly successful because of the distinctive features peculiar to HEMTs. In fact, although MESFETs and HEMTs admit the same small-signal equivalent circuit and exhibit both similar frequency behaviour for the scattering parameters and DC characteristics, some features are markedly different for HEMTs and MESFETs. Perhaps the most important discrepancy is the g_m compression at low gate bias, which is not observed in MESFETs and cannot be neglected, since P-HEMTs usually operate near the maximum gain bias points. A further discrepancy is found in the low-frequency dispersive behaviour: while in MESFETs the g_m degradates from DC to microwaves, in HEMTs no appreciable dispersion occurs between the threshold voltage and the maximum gain bias point, while the conductance increases versus frequency in the compression region. In order to account for the gain compression typical of HEMTs, modified Curtice and Materka approaches were first proposed [5]. Such models are somewhat difficult to correctly fit; a better empirical solution consists in the development of an entirely new model with built-in g_m compression, as suggested by Angelov et al. [1].

Model development and validation

In the present work, we considered the large-signal modelling of P-HEMTs for Ka-band medium-power amplifiers developed, manufactured and characterized by SIEMENS; the gate lengths are in the range 0.2-0.3 μm. As a modelling framework, the Angelov model was chosen after some preliminary evaluation of modified MESFET models [5]. In order to preserve flexibility, the model was implemented as a user-defined equation set within the framework of the HARPE/OSA [2] simulator, and the model structure was further refined through work on three successive generations of P-HEMTs which we shall denote hereafter as P-HEMT1, P-HEMT2 and P-HEMT3. The experience gained this way suggests that, unless black-box modelling approaches such as the Root model [6] or the modelling strategy proposed by Filicori et al. [4] are used, the most significant asset in a large-signal model is structure flexibility. Because of the continuous evolution of the technology, which brings about new effects in every device generation, accurate large-signal modelling cannot be possibly based on a fixed equation structure, but has to allow for adjustements in a flexible and user-friendly way. This is made possible by the use of large-signal modelling environments such as the HARPE simulator.

Starting the Angelov model structure, further effects, such as low-frequency dispersion, soft breakdown and finally DC current compression models based on device heating were allowed for; at the end of the process, an analytical model was obtained which yields very good agreement of the DC and small-signal parameters in a wide range of bias point. Preliminary large-signal measurements are also in good agreement. The model equations have been also exported into the MDS simulator, and will be used in this environment for circuit design. The lumped-parameter large-signal model implemented

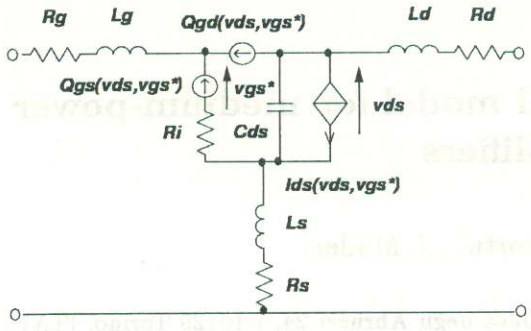

Figure 1: Structure of large-signal HEMT model.

is shown in Fig.1. A preliminary device (P-HEMT1) was taken first into consideration. The extraction of the DC and AC transconductance and output resistance revealed that the device was affected by a negligible amount of low-frequency dispersion; thus, satisfactory results were obtained through a straightforward implementation of the Angelov equations [1]:

$$I_{ds} = I_{pk} \cdot (1 + \tanh(\Psi)) \cdot (1 + \lambda V_{ds}) \cdot \tanh(\alpha V_{ds}),$$

where $\Psi = P_1\Delta + P_2\Delta^2 + P_3\Delta^3 + P_4\Delta^4 + P_5\Delta^5$, $\Delta = V_{gs} - V_{pk}$; V_{pk} is the voltage corresponding to the maximum g_m; P_1 and P_2 were initially set to zero in order to reduce the number of optimization parameters, since their influence turned out to be negligible. For the charge control model, the following equations were derived from the Angelov capacitance model:

$$\begin{aligned} Q_{gs} &= C_{gs0} \cdot (1 + \tanh(k_2 V_{ds}))(V_{gs} + \\ &+ \log(\cosh(k_1 V_{gs}))/k_1)) \\ Q_{dg} &= C_{gd0} \cdot (1 + \tanh(k_3 V_{gs})(V_{dg} + \\ &- \log(\cosh(k_4 V_{ds} + k_5 V_{ds} V_{gs}))/(k_4 + k_5 V_{gs})), \end{aligned}$$

but similar results were also obtained with a more conventional diode-like model.

A second device generation (P-HEMT2) was then considered, on the basis of an extended set of small-signal and DC measurements. These devices are characterized by a certain amount of soft breakdown effects, that were included in the model by means of the modified equations:

$$I_{ds} = I_{pk} \cdot (1 + \tanh(\Psi)) \cdot \tanh(\alpha V_{ds}) + a_{SBD} \cdot (V_{ds} - V_{gs})^3$$

where soft breakdown is taken care through the parameter a_{SBD}; this enables to remove the parameter "λ" previously introduced in the expression of I_{ds}. Thermal effects are also present for high currents and drain voltages; these were not included in the model, since the class A operating point and the dynamic load line fell into a region where current compression due to heating was negligible. The model was optimized through HARPE on the DC and scattering parameters measured

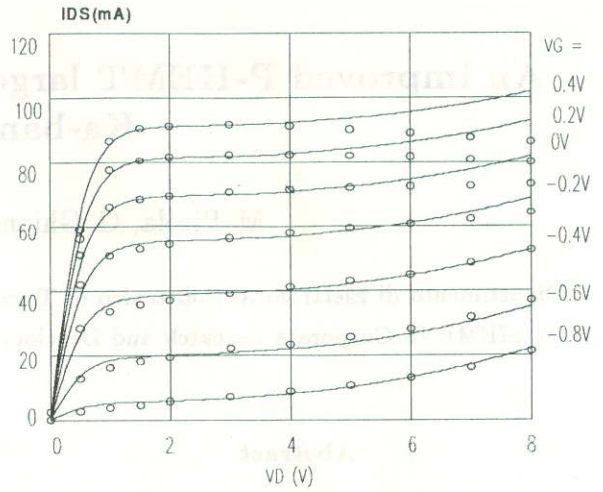

Figure 2: Measured and simulated DC curves of P-HEMT2 device.

in several working points on the frequency band 1-26 GHz. An example of the results obtained is shown in Fig.2 for the measured and simulated DC curves. Fig.3 shows the measured and simulated scattering parameters for the class A operating point; good agreement is also obtained for other bias points. Fig.4 and Fig.5 show the root mean square error on the frequency band 1-26 GHz between the measured and simulated scattering parameters, which is satsifactorily low in the class A operation region.

A final P-HEMT generation (P-HEMT3) was then considered. This device posed a challenging modelling problem, since it shows a fairly large amount of DC heating that partly compensates for the soft breakdown behaviour. This introduces considerable low-frequency dispersion of the transconductance and output resistance. The model equations were further modified so as to introduce a current compression due to heating (that is, the drain current has been made inversely proportional to the dissipated power in the saturation region), while low-frequency dispersion was accounted for by introducing a dynamic transconductance and output resistance. This is easily managed in HARPE and MDS simulators, since in those both the DC and the AC values of the driving voltages are available within the model. The final model equations in the HARPE implementation are:

```
!*************** drain current ******************
  VPK=VP + LL*VDS_T;
  PSI=P1*(VGS_TAU-VPK) + P2*(VGS_TAU-VPK)^2 +
      P3*(VGS_TAU-VPK)^3 + P4*(VGS_TAU-VPK)^4 +
      P5*(VGS_TAU-VPK)^5;
  VDG_T = S1*VDS_T + S2*VDS_T^2 +
          S3*VGS_T + S4*VGS_T^2;
  IDSNT=(IPK*(1+TANH(PSI)))*TANH(ALFA*VDS_T)*
        (1 + A1*VDG_T + A2*VDG_T^2 + A3*VDG_T^3
           + A4*VDG_T^4 + A5*VDG_T^5);
  GMAC=BETA*VDSDC*IDSNT;
  GDAC=R2*VGSDC^2 + R1*VGSDC + RO;
```

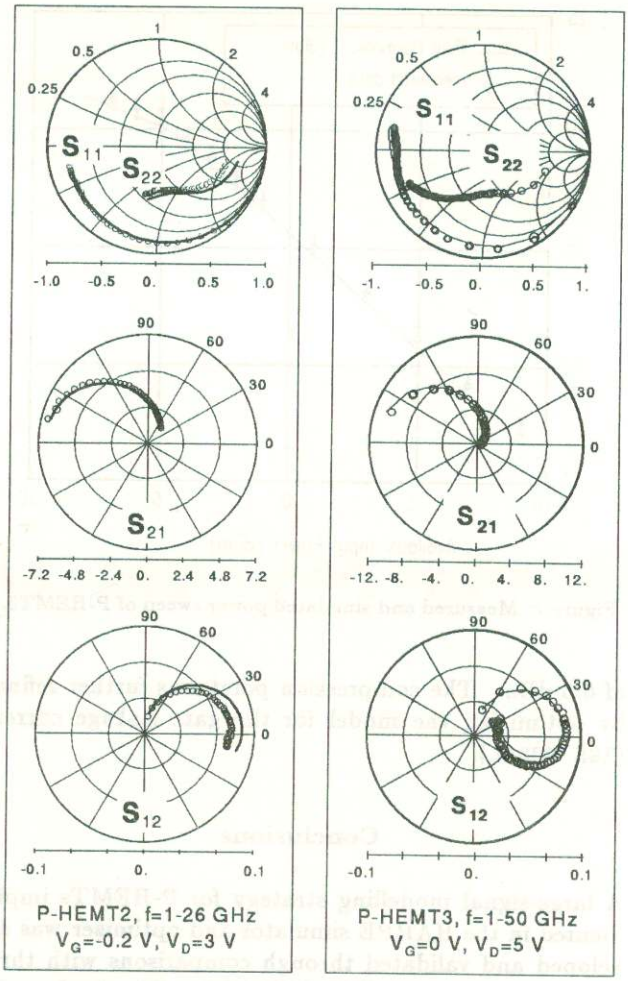

Figure 3: Examples of measured and simulated scattering parameters of P-HEMT2 and P-HEMT3 devices.

```
   RDSOW=1/GDSAC;
   IDS_MODEL=IDSNT/
         (1 + (KTH*ABS(VDS_T*IDSNT))^CHI) +
         (VDS_T-VDSDC)/RDSOW + (VGS_T-VGSDC)*GMAC;
!************ intrinsic resistance current ********
   IRIN_MODEL =(VGS_T - VGG_T) / RIN ;
!*************** drain-gate current **************
   IDG_MODEL =0 ;
!*************** gate-source current *************
   IGS_MODEL = IF (VGS_T > VBI)
               ((VGS_T - VBI) / RF);
!****************** gate charge ******************
   QGG_MODEL = CGSO*(1+TANH(K2*VDS_T))
               *(VGG_T+LOG(COSH(K1*VGG_T))/K1);
!*************** gate-drain charge ***************
   QDG_MODEL = CGDO*(1+TANH(K3*VGG_T))
               *(VDG_T-LOG(COSH(K4*VDS_T+K5
               *VDS_T*VGG_T))/(K4+K5*VGG_T));
```

The variables VDS_T and so forth are instantaneous values, while VDSDC etc. are the DC values (VDS_TAU etc. are delayed instantaneous values). In order to carry out the model fitting on the DC and scattering parameters, the model parameters were divided into two classes: those mainly influencing the DC behaviour, and those

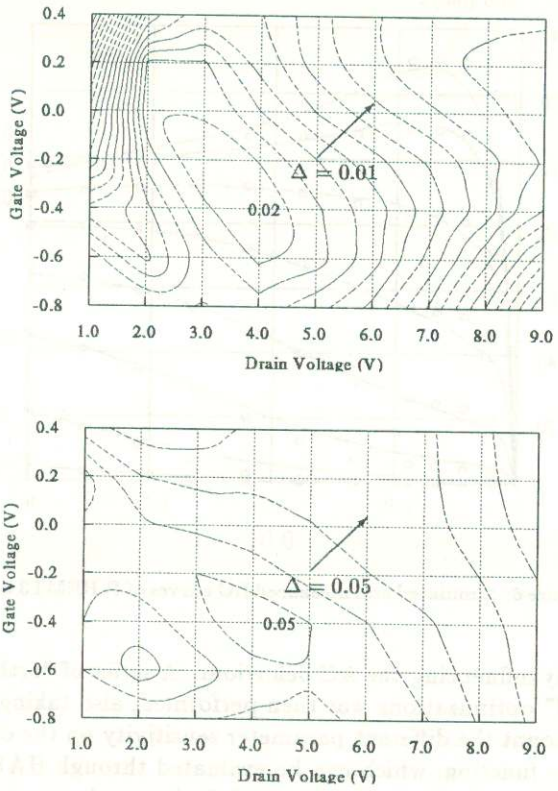

Figure 4: Error contours (see text) for S_{11}, S_{22} (from top to bottom); P-HEMT2 device.

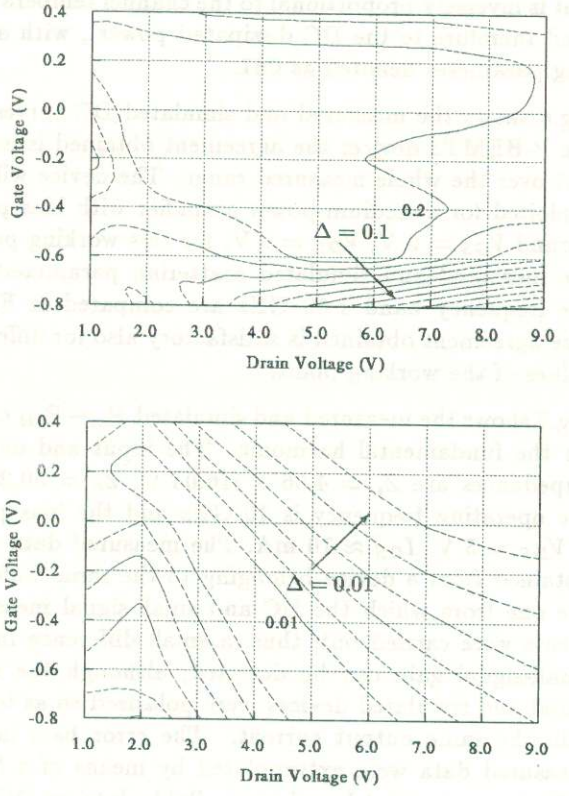

Figure 5: Error contours (see text) for S_{21}, S_{12} (from top to bottom); P-HEMT2 device.

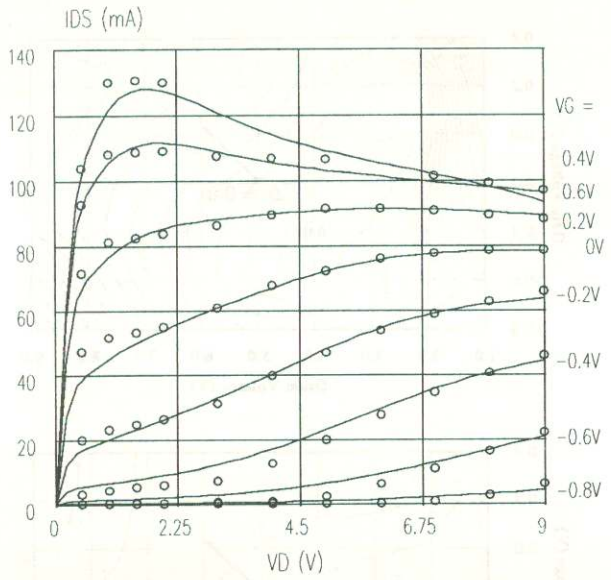

Figure 6: Simulated and measured DC curves of P-HEMT3 device.

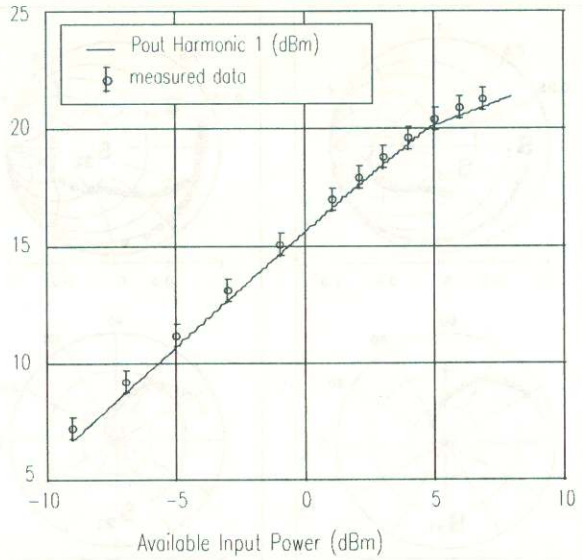

Figure 7: Measured and simulated power sweep of P-HEMT3.

only influencing the AC behaviour. A series of "orthogonal" optimizations was then performed, also taking into account the different parameter sensitivity on the objective function, which can be evaluated through HARPE. The form of the equation exploited was also suggested by physical insight gained from the behaviour of the extracted small-signal parameter in several working points. The heating model approximately assumes that the current is inversely proportional to the channel temperature (and therefore to the DC dissipated power), with a fitting parameter denoted as `CHI`.

Fig.6 shows the measured and simulated DC curves for the P-HEMT3 device; the agreement obtained is excellent over the whole measured range. The device will be exploited for a medium-power amplifier with bias point around $V_{GS} = 0$ V, $V_{DS} = 5$ V; for this working point, the measured and simulated scattering parameters on the frequency band 1-50 GHz are compared in Fig.3. The agreement obtained is satisfactory also for different values of the working point.

Fig.7 shows the measured and simulated $P_{in} - P_{out}$ curve for the fundamental harmonic. The input and output impedances are $Z_i = 4.66 + j16.04\ \Omega$, $Z_o = 50.27\ \Omega$, the operating frequency is 10 GHz and the bias point is $V_{DS} = 5$ V, $I_{DS} \approx 70$ mA. The measured data were obtained from a device belonging to the same wafer as the one from which the DC and small-signal measurements were carried out; thus, a small difference in the small-signal gain can be detected, although the measured and simulated devices were polarized so as to obtain the same output current. The error bars in the measured data were extrapolated by means of a MonteCarlo scatter plot based on available data on DC and small-signal parameter uniformity, and refer to the estimated standard deviation which turns out of the order of 0.5 dBm. The compression point was further refined by optimizing the model for the gate leakage current (`IGS_MODEL`).

Conclusions

A large-signal modelling strategy for P-HEMTs implemented in the HARPE simulator and optimizer was developed and validated through comparisons with three generations of SIEMENS P-HEMTs. The final model has been exported into MDS and will be exploited for circuit design. Future work will concern an extended validation carried out on harmonic power sweep measurements and load-pull measurements.

Acknowledgements. This work was partly supported by the ESPRIT 6050 "MANPOWER" project.

References

[1] Angelov et al., "A new empirical nonlinear model for HEMT and MESFET devices", *IEEE Transaction on Microwave Theory & Techniques*, vol. 40, December 1992, pp. 2258÷2266.

[2] OSA90/hope. Distributed by: Optimization Systems Associates Inc., Dundas, Ontario, Canada.

[3] MDS - HP 85150B Microwave and RF Design Systems. Distributed by: Hewlett Packard.

[4] F.Filicori, G.Vannini and V.A.Monaco, "A nonlinear integral model of electron devices for HB circuit analysis", in SPICE", *IEEE Transactions Microwave Theory & Techniques*, pp. 1456÷1465, July 1992

[5] J.M. Golio, *Microwave MESFETs & HEMTs*, Artech House, 1991.

[6] D.E.Root, S.Fan and J.Meyer, "Technology independent non quasi-static FET models by direct construction from automatically characterized device data", *Proc. of 21st European Microwave Conference*, pp.927-932, September 1991.